Organic Electronics 13 (2012) 1004–1011

Contents lists available at SciVerse ScienceDirect

Organic Electronics

journal homepage: www.elsevier.com/locate/orgel

Effect of hydroxyl density on condensation behaviors of self-assembled monolayers and performance of pentacene-base organic thin-film transistors

Hsin-Chieh Tiao [a], Yao-Jen Lee [b], Yi-Shan Liu [a], Shu-Hsien Lee [a], Ching-Hsiu Li [a], Ming-Yu Kuo [a,*]

[a] Department of Applied Chemistry, National Chi Nan University, Puli, Nantou, Taiwan
[b] National Nano Device Laboratories, Hsinchu, Taiwan

ARTICLE INFO

Article history:
Received 8 December 2011
Received in revised form 7 February 2012
Accepted 6 March 2012
Available online 17 March 2012

Keywords:
Organic field-effect transistors
Self-assembled monolayer
Pentacene
O_2 plasma
Preparing temperature

ABSTRACT

A series of self-assembled monolayers (SAMs), comprising octadecyltrichlorosilane (ODTS), dodecyltrichlorosilane (DDTS), and hexamethyldisilazane (HMDS), were prepared to examine the effects of phase states and condensation behaviors of SAMs on the morphologies and performance of pentacene-based organic field-effect transistors (OFETs) by means of Fourier Transform Infrared (FT-IR) spectrometer, atomic force microscope (AFM), X-ray diffraction (XRD), and semiconductor parameter analyzer. Experimental results reveal that the treatment of SiO_2 substrates with O_2 plasma (denoted as O_2-SiO_2) and the preparation temperature of SAMs dramatically influence the morphologies of SAMs and the performance of corresponding pentacene-based (no purification) OFETs. When the SAMs were prepared at 30 °C, the OFET based on ODTS-treated O_2-SiO_2 substrate had the highest hole mobility, reaching as large as 1.15 $cm^2 V^{-1} s^{-1}$, and an on/off current ratio in excess of 10^5; these values are both much larger than those of a device based on ODTS-modified SiO_2 substrates without O_2 plasma treatment and O_2-SiO_2 substrates modified by ODTS SAMs prepared at other temperatures. OFETs based on O_2-SiO_2 substrates that were modified by DDTS and HMDS SAMs prepared at 4 °C performed best.

1. Introduction

Pentacene-based organic field-effect transistors (OFETs) have received substantial interest in recent decades, owing to their high hole mobility and on/off current ratio [1–45], which are comparable to those of commercially amorphous silicon-base FETs. The performance of pentacene-based OFETs depends significantly on the molecular order, morphology, and grain boundary within the active layer, which can be effectively controlled by varying the wafer cleaning procedures [1–4], deposition rate of pentacene [5], substrate temperature [5–7], and modification of the self-assembled monolayer (SAM) [6–25] or polymeric ultrathin films [21,26–41] on the substrate. The phase states of SAMs are critical to improving the molecular order within the active layer and the performance of OFETs [7,15–17]. Bao et al. presented a simple technique for fabricating an ultrasmooth octadecyltrimethoxysilane (ODTMS) SAM on UV/ozone-cleaned SiO_2 substrate by spin-coating, resulting in high-performance OFETs based on penatcene and C_{60} [16]. In 1994, Rondelez et al. systematically studied the relationship between the molecular structure in a series of *n*-alkyltrichlorosilane SAMs and the temperature of preparation [46–47]. They determined the transition temperature T_c at which ordered *n*-alkyltrichlorosilane SAMs on SiO_2 substrates were formed by making contact angle and Fourier transform infrared (FT-IR) measurements. This transition temperature T_c for octadecyltrichlorosilane (ODTS), one of the most studied

* Corresponding author. Address: Department of Applied Chemistry, National Chi Nan University, No. 1 University Rd., 545 Puli, Nantou, Taiwan. Fax: +886 49 2917956.
E-mail address: mykuo@ncnu.edu.tw (M.-Y. Kuo).

1566-1199/$ - see front matter © 2012 Elsevier B.V. All rights reserved.
http://dx.doi.org/10.1016/j.orgel.2012.03.004

SAMs, is around 28 ± 5 °C. Below T_c, ODTS forms an ordered SAM on the SiO_2 substrate while the ODTS SAM is disordered above T_c. Cho et al. showed that such ordered and disordered ODTS SAMs dramatically affect the performance of pentacene-based OFETs [7]. They found that the hole mobility of an OFET based on pentacene films deposited on ordered ODTS SAMs prepared at 4 °C are much higher than those deposited on disordered ODTS SAMs prepared at 65 °C.

Previously, Rye commented on the investigation of Rondelez et al., who found that the formation of ordered *n*-alkyltrichlorosilane SAMs depends on strong covalent bonds between the anchoring groups of *n*-alkyltrichlorosilane and hydroxyl (–OH) groups on SiO_2 surface, as well as on the van der Waals' interaction between the alkane chains [48]. Numerous studies have demonstrated that O_2 plasma treatment can remove residual organic contamination and increase the density of hydroxyl groups on the oxide surface, enhancing the covalent bonds between the SAM molecules and the oxide surface [49–51]. Hsieh et al. revealed that ultrasmooth ODTS SAMs can be formed by the treatment of SiO_2 substrate with O_2 plasma using low polarity solvents, such as hexadecane and toluene [51]. Cho et al. investigated the effect of preparation temperature of ODTS SAMs on the performance of OFETs based on SiO_2 substrates without O_2 plasma treatment [7]. However, the influence of hydroxyl density of the SiO_2 substrate on the phase states of *n*-alkyltrichlorosilane SAMs prepared at different temperatures and the performance of OFETs based on such films have not been fully studied.

This study investigates the phase states and condensation behaviors of a series of silane-based SAMs on SiO_2 substrates that were prepared at various temperatures of SAMs and with different hydroxyl densities, controlled by O_2 plasma treatment. The effects of these factors on the morphology of pentacene (no purification) and the performance of OFETs based on such films were also explored. Experimental results indicate that the OFET based on O_2 plasma-treated SiO_2 (O_2-SiO_2) that was immersed in a 5 mM toluene solution of ODTS at 30 °C for 6 h has a hole mobility of as high as 1.15 $cm^2 V^{-1} s^{-1}$ and an on/off current ratio in excess of 10^5, which values are much larger than those of devices based on ODTS-modified SiO_2 substrates without O_2 plasma treatment and O_2-SiO_2 substrates modified by ODTS SAMs prepared at other temperatures. SiO_2 substrates that had and had not undergone O_2 plasma treatment were denoted as O_2-SiO_2 and N-SiO_2 substrates, respectively. Pentacene thin films based on SAMs prepared at 4, 30, and 60 °C were designated PENT4, PENT30, and PENT60, respectively.

2. Experimental

2.1. Materials

Octadecyltrichlorosilane (ODTS, 95%, purchased from Acros), dodecyltrichlorosilane (DDTS, 97%, purchased from TCI), hexamethyldisilazane (HMDS, 98%, purchased from Acros), anhydrous toluene (Acros), and pentacene (Sigma–Aldrich) were used as received. OFET devices were made using heavily n-doped Si wafers as back gate electrodes with a thermally oxidized SiO_2 (270 nm, capacitance C_i = 11 nF cm^{-2}) dielectric. The substrate, soaked in piranha solution (concentrated H_2SO_4/30% H_2O_2 7:3 v/v) for 60 min, was cleaned using distilled water and dried in a flow of pure nitrogen. O_2-SiO_2 substrates were finally cleaned using PDC-32G plasma cleaner (Harrick) at low power for 1 min.

2.2. Preparation of self-assembled monolayer (SAM)

The substrates treated by self-assembled monolayers (SAMs) were prepared by immersing them into a 5 mM solution of SAMs in dry toluene for 6 h at different preparing temperatures (10–60 °C), controlled using a refrigerated circulator. Preparation temperatures of 4 and −10 °C were maintained in the cooler and freezer compartments of a refrigerator, respectively. Subsequently, the substrates were cleaned by ultrasonication in toluene and dried in flowing pure nitrogen. The SAM-treated substrates were baked at 120 °C in a vacuum oven for 1 h.

2.3. Characterization

The phase states of SAMs were investigated using Fourier transform Infrared (FT-IR) spectrometer (VERTEX 70). Atomic force microscope (AFM) images of pentacene films and SAM-treated substrates were obtained using Veeco Dimension 5000 scanning probe microscope. The inner structures of pentacene films were determined by X-ray diffraction (XRD, Rigaku 18 kW Rotating Anode X-ray Generator) using Cu K_α radiation ($\lambda_{K\alpha1}$ = 1.54 Å). Contact angle (CA) values of water were measure using Sindatek 100 SB.

2.4. OFET device fabrication

Pentacene films (45 nm) were thermally evaporated onto SAM-treated substrates at a rate of 0.1–0.2 Å s^{-1} under a pressure of 5×10^{-6} torr. The substrates were maintained at constant temperature of 65 °C. Finally, Au source-drain electrodes (60 nm) were thermally evaporated onto the pentacene films (top contact) through a shadow mask. The channel length (L) and width (W) are 100 μm and 2000 μm, respectively. All of the transistors were characterized under ambient air using an HP 4145B semiconductor parameter analyzer. The charge mobility (μ) was calculated from the saturation regime using the formula, $I_d = (WC_i/2L)\mu(V_g - V_{th})^2$, where L is the channel length; W is the channel width; C_i is the capacitance per unit area of SiO_2, I_d is the drain current, V_g is the gate voltage, and V_{th} is the threshold voltage.

3. Results and discussion

3.1. Phase states and condensation behaviors of ODTS

To investigate the molecular order of ODTS SAMs prepared under different conditions, their FT-IR spectra were obtained. Fig. 1 indicates that the molecular order of ODTS SAMs does not depend on the treatment of the SiO_2

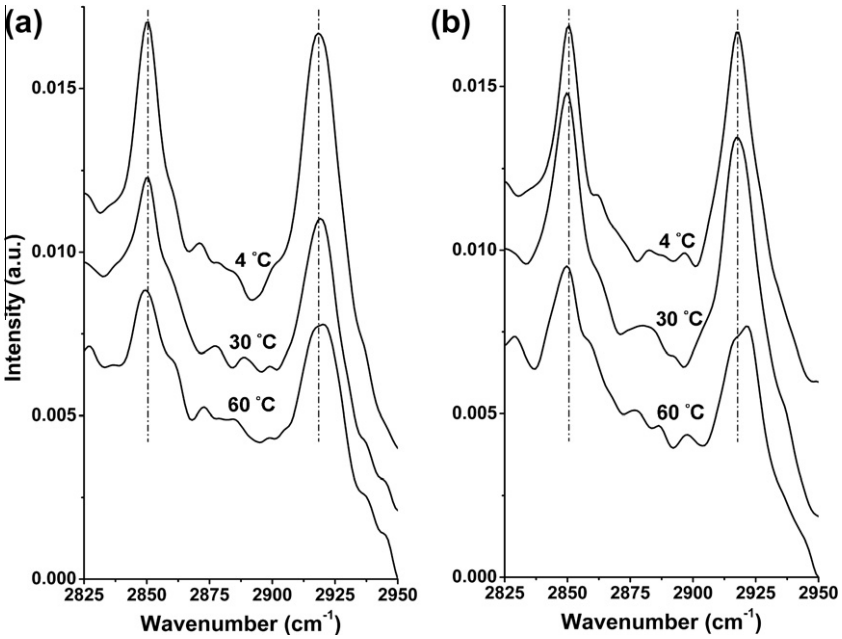

Fig. 1. FTIR spectra of ODTS SAMs prepared at different temperatures and SiO_2 substrates (a) N-SiO_2 and (b) O_2-SiO_2.

substrates with O_2 plasma. The ODTS SAMs on both types of SiO_2 substrates exhibit similar spectra at different preparation temperature of ODTS. Below 30 °C, the ODTS SAMs had ordered structures (all-trans -CH_2-); above 30 °C, they converted into disordered structures, as revealed by the upward shift of CH_2 stretching vibration [7,15–17]. The surface morphologies of ODTS SAMs were characterized by atomic force microscopy (AFM) as presented in Fig. 2. The ODTS SAMs on N-SiO_2 and O_2-SiO_2 substrates show similar morphologies when the SAMs were prepared at 4 and 60 °C. The ODTS SAMs exhibit dramatic aggregation on O_2-SiO_2 substrates. The morphologies of ODTS SAMs on these two substrates differ markedly at a preparation temperature of 30 °C. The ODTS SAMs on N-SiO_2 substrate have a very rough surface; however, they form a very smooth surface on O_2-SiO_2 substrate. Fig. 3 presents a simple scheme of several conditions of ODTS SAMs to explain this phenomenon. The condensation behaviors of ODTS SAMs vary with preparation conditions probably because of the variation in density of the hydroxyl groups of SiO_2 substrates and the different solubility of ODTS in toluene. The solubility of ODTS in toluene at 4 °C is lower than that at 30 °C. The ODTS molecules aggregate at 4 °C before and after anchoring onto N-SiO_2 (Fig. 3a) and O_2-SiO_2 substrates. Therefore, the rough surface was formed. The lower solubility of ODTS in toluene at 4 °C can be proven by the formation of gel after 6 h of deposition (Fig. 4), whereas the ODTS solution remains clear at 30 °C during the same period. The ODTS forms a smooth monolayer structure on O_2-SiO_2 substrate at 30 °C owing to the sufficient number and uniform density of the hydroxyl groups (Fig. 3b). However, the density of hydroxyl groups on N-SiO_2 surface is insufficient to form a uniform monolayer at this temperature. Such difference of hydroxyl density can be proven by the reduced CA values of bare SiO_2 substrates from 29° to 17° (Fig. 1S) after treatment with O_2 plasma. Wherefore when the first few ODTS molecules anchor onto the limited number of silanol groups, the following condensation can occur between ODTs molecules (Fig. 3c). The unanchored aggregations of ODTS molecules were rinsed off after ultrasonication. Finally, the rough surface was observed on N-SiO_2 substrate at 30 °C. The FT-IR spectra and AFM images indicate that the ordered (all-trans -CH_2-) ODTS molecules aggregate on the N-SiO_2 substrates at both 4 and 30 °C and on the O_2-SiO_2 substrate at 4 °C. The ordered ODTS molecules form a smooth monolayer on the O_2-SiO_2 substrate at 30 °C.

3.2. Performance of organic field-effect transistors

Top-contact OFETs were fabricated to explore the effect of phase states of ODTS SAMs on the performance of the corresponding pentacene-based OFETs. Other preparation temperatures of ODTS SAMs on O_2-SiO_2 substrates were tested to optimize the fabrication conditions. Table 1 shows the charge mobilities and on/off current ratios of these devices fabricated on both N-SiO_2 and O_2-SiO_2 substrates. On N-SiO_2 substrates, PENT4 and PENT30 perform quite similarly, consistent with FT-IR and AFM results. The conversion of SAMs from an ordered to a disordered state drastically reduces the charge mobility of PENT60. These results are consistent with those of Cho et al. [7]. On O_2-SiO_2 substrates, the performance of PENT60 is similar with that on N-SiO_2 substrate prepared at the same temperature; however, the trend of performance of OFETs based on ODTS SAMs prepared between 4 and 30 °C is different from those fabricated on N-SiO_2 substrates. The maximum charge mobility and on/off current ratio of PENT4 based on

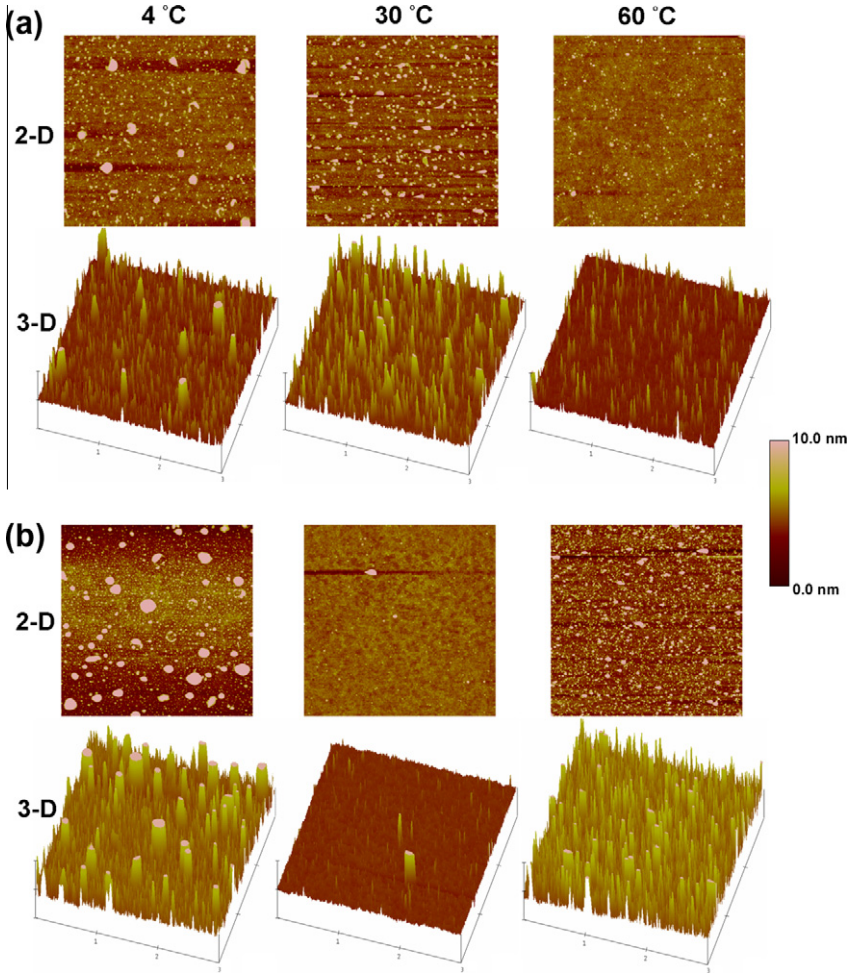

Fig. 2. AFM images (3 μm × 3 μm) of ODTS SAMs prepared at different temperatures (a) N-SiO_2 substrates and (b) O_2-SiO_2 substrates.

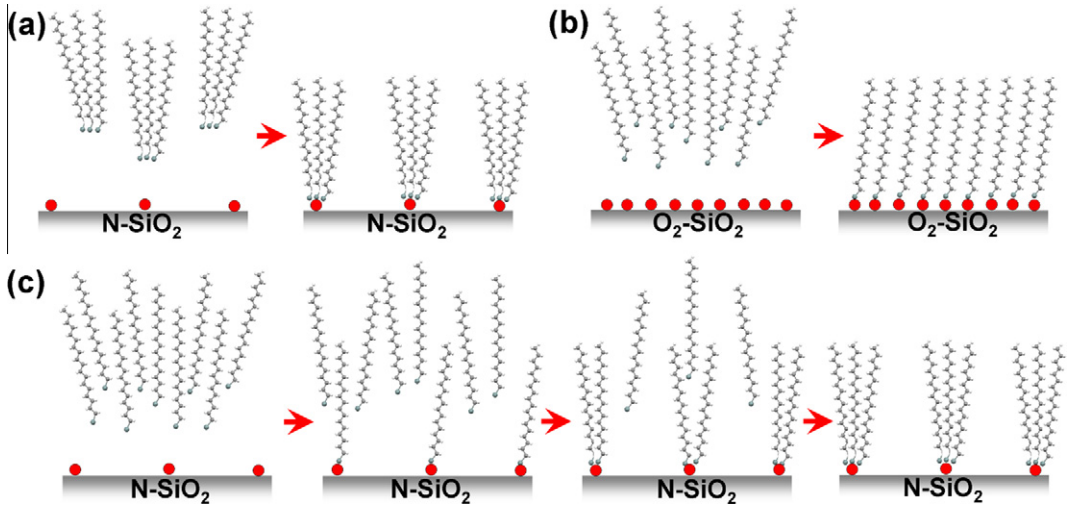

Fig. 3. Condensation behaviors of ODTS SAMs at different conditions (a) 4 °C on N-SiO_2, (b) 30 °C on O_2-SiO_2 and (c) 30 °C on N-SiO_2. The red circles present the hydroxyl groups on the SiO_2 substrates. (For interpretation of the references to colour in this figure legend, the reader is referred to the web version of this article.)

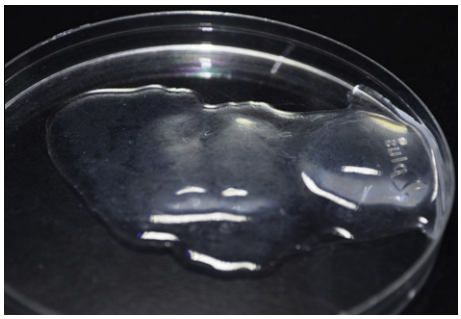

Fig. 4. The gel of ODTS in toluene at 4 °C after 6 h of deposition.

Table 1
The electrical characteristics of pentacene-based OFETs on ODTS SAMs measured in ambient conditions. The μ_{ave} values are the averages of 10 channels for each OFET.

Substrate	Device	μ_{ave} ($cm^2\ V^{-1}\ s^{-1}$)	μ ($cm^2\ V^{-1}\ s^{-1}$)	I_{on}/I_{off}
N-SiO_2	PENT4	0.597	0.492 ~ 0.669	1.42×10^5
	PENT30	0.503	0.468 ~ 0.528	1.79×10^5
	PENT60	0.100	0.079 ~ 0.115	3.62×10^4
O_2-SiO_2	PENT4	0.291	0.250 ~ 0.309	7.84×10^4
	PENT25	0.467	0.396 ~ 0.508	1.29×10^5
	PENT27.5	0.631	0.540 ~ 0.695	1.80×10^5
	PENT30	1.010	0.846 ~ 1.150	2.06×10^5
	PENT30 (55)[a]	0.746	0.657 ~ 0.833	1.59×10^5
	PENT30 (90)[b]	0.735	0.635 ~ 0.835	2.48×10^5
	PENT32.5	0.630	0.585 ~ 0.739	1.48×10^5
	PENT35	0.339	0.301 ~ 0.372	7.76×10^4
	PENT60	0.068	0.061 ~ 0.069	1.18×10^4

[a] Substrate temperature at 55 °C.
[b] Substrate temperature at 90 °C.

O_2-SiO_2 substrate are only 0.309 $cm^2\ V^{-1}\ s^{-1}$ and 7.84×10^4, respectively. From 4 to 30 °C, the performance of OFETs based on O_2-SiO_2 substrate is proportional to the preparation temperature of ODTS SAMs. The maximum hole mobility and on/off current ratio of PENT30 based on O_2-SiO_2 substrate exceed 1 $cm^2\ V^{-1}\ s^{-1}$ and 2×10^5, respectively. From 30 to 60 °C, however, the performance of OFETs based on O_2-SiO_2 substrates is inversely proportional to the preparation temperatures of ODTS SAMs. The maximum hole mobility and on/off current ratio of PENT60 based on O_2-SiO_2 substrate are more than an order of magnitude lower than those of PENT30. Fig. 5 plots selected *I-V* curves. To optimize the performance of OFET, the pentacene films based on the ODTS SAMs prepared at 30 °C (PENT30) were also deposited at substrate temperatures of 55 and 90 °C (Table 1). The results indicate that PENT30 with a substrate temperature of 65 °C performs best. To explore the effect of the preparation conditions of ODTS SAMs on the performance of OFETs, the morphologies and molecular order of some important pentacene films based on ODTS SAMs were characterized by AFM and X-ray diffraction (XRD) as given in Figs. 6 and 7, respectively. The AFM images of PENT4 and PENT30 based on N-SiO_2 substrates show that they have similar textures of small terraces. The corresponding XRD patterns of these two films are dominated by the thin film phase layer structures ((00 1′) at $2\theta = 5.75°$), but also include weak signals from bulk phase layer structures ((00 1) at $2\theta = 6.17°$). Accordingly, these two OFETs perform almost equally. However, the preparation temperature of ODTS SAMs on O_2-SiO_2 substrates dramatically affects the morphologies of following pentacene films. The grains in PENT30 are much larger than those in PENT4. The corresponding XRD patterns of both pentacene films reveal only pure thin film phase layer structures; the XRD intensity of PENT30 is almost ten times that of PENT4, which is consistent with the *I-V* measurements. The AFM images and XRD patterns of PENT60 based on disordered ODTS SAMs on both N-SiO_2 and O_2-SiO_2 substrates show very roughly discontinuous 3D islands and weak bulk phase layer structures, respectively. These discontinuous morphologies explain why the performance of the corresponding OFETs is very poor. Since the transition temperature T_c depends on the chain length of *n*-alkyltrichlorosilane [46], the effects of the preparation temperatures of dodecyltrichlorosilane (DDTS) and hexamethyldisilazane (HMDS) on the hole mobility of pentacene-based OFETs on O_2-SiO_2 substrates were also investigated (Table 2). Again, the performance of pentacene-based OFETs on both SAMs varied with the preparation temperature of the SAMs. The PENT4 devices based on DDTS and HMDS SAMs had the highest hole mobilities of 0.726 and 0.559 $cm^2\ V^{-1}\ s^{-1}$, respectively,

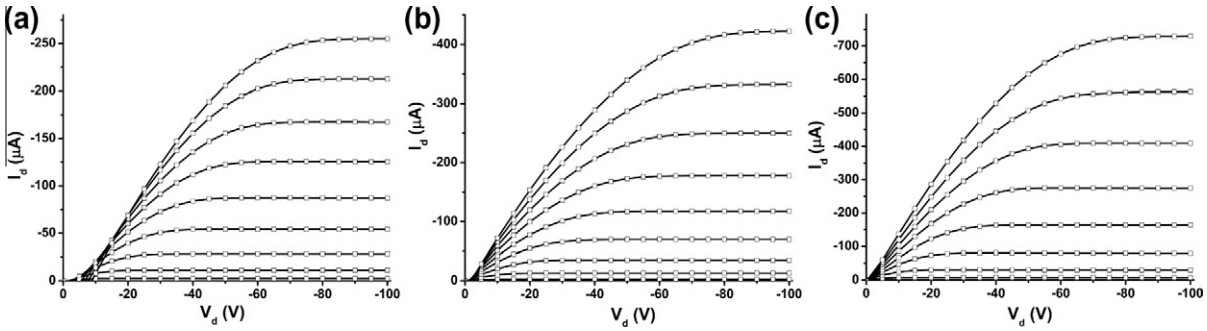

Fig. 5. Output characteristics of selected pentacene-based OFETs on ODTS SAMs (a) PENT4 on O_2-SiO_2 substrate (b) PENT30 on N-SiO_2 substrate and (c) PENT30 on O_2-SiO_2 substrate. Gate voltage from 0 to −100 V.

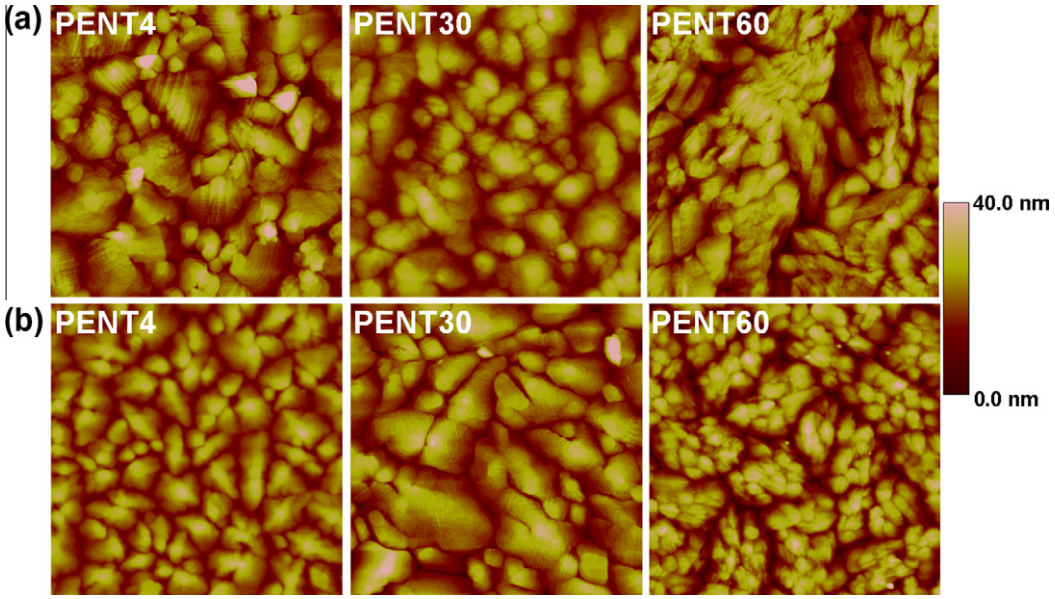

Fig. 6. AFM images (3 μm × 3 μm) of pentacene films based on ODTS SAMs prepared at different temperatures (a) N-SiO_2 substrates and (b) O_2-SiO_2 substrates.

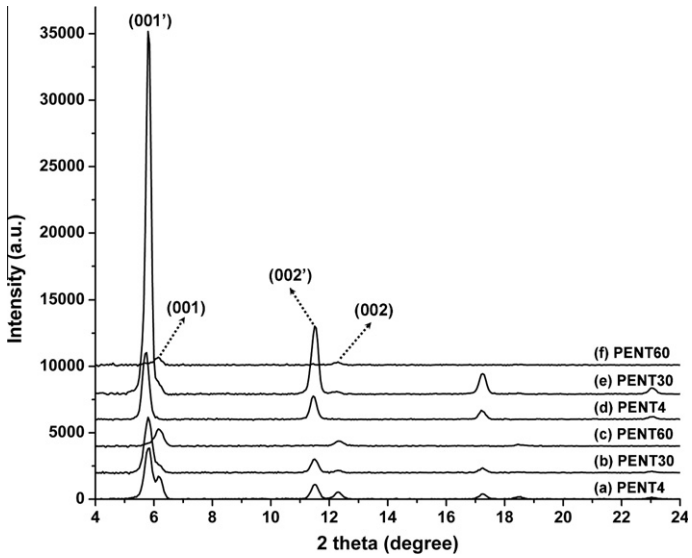

Fig. 7. XRD patterns of pentacene films based on ODTS SAMs prepared at different temperatures and SiO_2 substrates (a)–(c) N-SiO_2 substrates and (d)–(f) O_2-SiO_2 substrates.

which consistent with the AFM images of DDTS and HMDS SAMs (Fig. 2S) and XRD patterns of pentacene films based on these substrates (Fig. 3S). For both DDTS and HMDS, the SAMs prepared at 4 °C show the smoother morphologies and the corresponding XRD patterns of PENT4 films display stronger intensities than those prepared at other temperatures. Fig. 8 summarizes the highest hole mobilities of pentacene-based OFETs on three SAMs prepared at various temperatures. It can be see that the performance of pentacene-based OFETs is very sensitive to the preparation temperature of the SAMs. For ODTS, the best performance of OFET was fabricated on the SAM prepared at 30 °C, which is consistent with the transition temperature T_c (28 ± 5 °C) of ODTS [46]. Rondelez et al. showed that the transition temperatures T_c of *n*-alkyltrichlorosilane SAMs have a shift of 3.5 ± 5 °C per CH_2 unit. For DDTS, the transition temperature T_c is around 6 °C; therefore, the PENT4 device based on this SAM performs best. For nonlinear HMDS, the PENT4 device also shows the best performance.

Table 2
The electrical characteristics of pentacene-based OFETs on DDTS and HMDS SAMs measured in ambient conditions. The μ_{ave} values are the averages of 10 channels for each OFET.

SAM	Device	μ_{ave} ($cm^2\,V^{-1}\,s^{-1}$)	μ ($cm^2\,V^{-1}\,s^{-1}$)	I_{on}/I_{off}
DDTS	PENT-10	0.194	0.146–0.226	5.58×10^4
	PENT4	0.675	0.634–0.726	1.75×10^5
	PENT10	0.641	0.598–0.722	2.61×10^5
	PENT20	0.627	0.553–0.658	3.85×10^5
	PENT30	0.609	0.561–0.652	2.16×10^5
	PENT40	0.513	0.431–0.581	1.88×10^4
HMDS	PENT-10	0.079	0.065–0.092	2.96×10^5
	PENT4	0.493	0.403–0.559	1.26×10^6
	PENT10	0.464	0.412–0.520	2.96×10^5
	PENT20	0.190	0.157–0.243	5.85×10^4

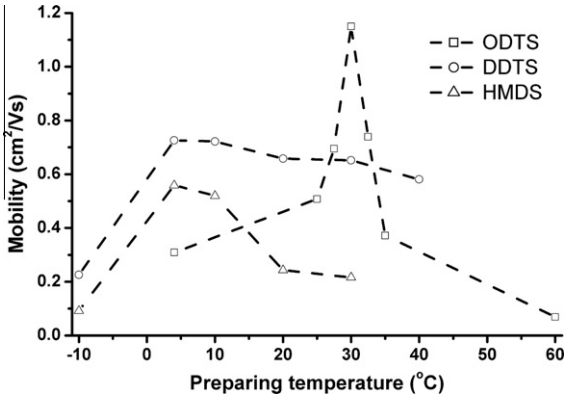

Fig. 8. Hole mobility of OFET with respect to chain length and preparation temperature of SAMs.

4. Conclusion

In conclusion, this study investigated the phase states and condensation behaviors of a series of self-assembled monolayers (SAMs)- octadecyltrichlorosilane (ODTS), dodecyltrichlorosilane (DDTS) and hexamethyldisilazane (HMDS) -on SiO_2 substrates with different hydroxyl densities controlled by O_2 plasma treatment. Experimental results reveal that both the preparation temperatures of SAMs and the hydroxyl density of the SiO_2 substrates significantly affect the morphologies of SAMs and the performance of corresponding pentacene-based (no purification) OFETs. An OFET that was based on O_2 plasma-treated SiO_2 (O_2-SiO_2) substrate immersed in a 5 mM toluene solution of ODTS at 30 °C for 6 h had a hole mobility of as large as 1.15 $cm^2\,V^{-1}\,s^{-1}$ and an on/off current ratio of over 10^5, which values considerably exceed those of devices based on ODTS-modified SiO_2 substrates without O_2 plasma treatment and O_2-SiO_2 substrates that were modified by ODTS SAMs prepared at other temperatures. OFETs based on O_2-SiO_2 substrates that were modified by DDTS and HMDS SAMs prepared at 4 °C performed best.

Acknowledgment

This work was supported by the National Science Council of Taiwan (NSC-98-2113-M-260-001 and 99-2113-M-260-007-MY3).

Appendix A. Supplementary data

Supplementary data associated with this article can be found, in the online version, at http://dx.doi.org/10.1016/j.orgel.2012.03.004.

References

[1] B.J. Song, K. Hong, W.K. Kim, K. Kim, S. Kim, J.L. Lee, Effect of oxygen plasma treatment on crystal growth mode at pentacene/ni interface in organic thin-film transistors, J. Phys. Chem. B 114 (2010) 14854–14859.
[2] J.W.H. Smith, I.G. Hill, Influence of SiO_2 dielectric preparation on interfacial trap density in pentacene-based organic thin-film transistors, J. Appl. Phys. 101 (2007) 044503.
[3] W.K. Kim, K. Hong, J.L. Lee, Enhancement of hole injection in pentacene organic thin-film transistor of O_2 plasma-treated Au electrodes, Appl. Phys. Lett. 89 (2006) 142117.
[4] Q. Qi, A. Yu, P. Jiang, C. Jiang, Enhancement of carrier mobility in pentacene thin-film transistor on SiO_2 by controlling the initial film growth modes, Appl. Surf. Sci. 255 (2009) 5096–5099.
[5] M. Shtein, J. Mapel, J.B. Benziger, R. Forrest, Effects of film morphology and gate dielectric surface preparation on the electrical characteristics of organic-vapor-phase-deposited pentacene thin-film transistors, Appl. Phys. Lett. 81 (2002) 268–270.
[6] S. Steudel, D. Janssen, S. Verlaak, J. Genoe, P. Heremans, Patterned growth of pentacene, Appl. Phys. Lett. 85 (2004) 5550–5552.
[7] H.S. Lee, D.H. Kim, J.H. Cho, M. Hwang, Y. Jang, K. Cho, Effect of the phase states of self-assembled monolayers on pentacene growth and thin-film transistor characteristics, J. Am. Chem. Soc. 130 (2008) 10556–10564.
[8] T.W. Kelly, L.D. Boardman, T.D. Dunbar, D.V. Muyres, M.J. Pellerite, T.P. Smith, High-performance OTFTs using surface-modified alumina dielectrics, J. Phys. Chem. B 107 (2003) 5877–5881.
[9] C. Bock, D.V. Pham, U. Kunze, D. Käfer, G. Witte, Ch. Wöll, Improved morphology and charge carrier injection in pentacene field-effect transistors with thiol-treated electrodes, J. Appl. Phys. 100 (2006) 114517.
[10] D. Knipp, R.A. Street, A. Völkel, J. Ho, Pentacene thin film transistors on inorganic dielectrics: morphology, structural properties, and electronic transport, J. Appl. Phys. 93 (2003) 347–355.
[11] S. Kobayashi, T. Nishikawa, T. Takenobu, S. Mori, T. Shimoda, T. Mitani, H. Shimotani, N. Yoshimoto, S. Ogawa, Y. Iwasa, Control of carrier density by self-assembled monolayers in organic field-effect transistors, Nat. Mater. 3 (2004) 317–322.
[12] F.D. Fleischli, S. Suárez, M. Schaer, L. Zuppiroli, High-performance OTFTs using surface-modified alumina dielectrics, Langmuir 26 (2010) 15044–15049.
[13] H.S. Seo, Y.S. Jang, Y. Zhang, P.S. Abthagir, J.H. Choi, Fabrication and characterization of pentacene-based transistors with a room-temperature mobility of 1.25 cm^2/Vs, Org. Electron. 9 (2008) 432–438.
[14] A. von Mühlenen, M. Castellani, M. Schaer, L. Zuppiroli, Controlling charge-transfer at the gate interface of organic field-effect transistors, Phys. Stat. Sol. 245 (2008) 1170–1174.
[15] D.H. Kim, H.S. Lee, H. Yang, L. Yang, K. Cho, Tunable crystal nanostructures of pentacene thin films on gate dielectrics possessing surface-order control, Adv. Funct. Mater. 18 (2008) 1363–1370.
[16] Y. Ito, A.A. Virkar, S. Mannsfeld, J.H. Oh, M. Toney, J. Locklin, Z. Bao, Crystalline ultrasmooth self-assembled monolayers of alkylsilanes for organic field-effect transistors, J. Am. Chem. Soc. 131 (2009) 9396–9404.
[17] A. Virkar, S. Mannsfeld, J.H. Oh, M.F. Toney, Y.H. Tan, G.Y. Liu, J.C. Scott, R. Miller, Z. Bao, The role of OTS density on pentacene and C60 nucleation, thin film growth, and transistor performance, Adv. Funct. Mater. 19 (2009) 1962–1970.
[18] S.M. Jeong, J.W. Park, Monolayers of twisted binaphthyls for aromatic crystallization at low nucleation densities and high growth rates, J. Am. Chem. Soc. 130 (2008) 3497–3501.

[19] H. Yang, T.J. Shin, M.M. Ling, K. Cho, C.Y. Ryu, Z. Bao, Conducting AFM and 2D GIXD studies on pentacene thin films, J. Am. Chem. Soc. 127 (2005) 11542–11543.
[20] K.C. Liao, A.G. Ismail, L. Kreplak, J. Schwartz, I.G. Hill, Designed organophosphonate self-assembled monolayers enhance device performance of pentacene-based organic thin-film transistors, Adv. Mater. 22 (2010) 3081–3085.
[21] A. Facchetti, M.H. Yoon, T.J. Marks, Gate dielectrics for organic field-effect transistors: new opportunities for organic electronics, Adv. Mater. 17 (2005) 1705–1725.
[22] O. Acton, M. Dubey, T. Weidner, K.M. O'Malley, T.W. Kim, G.G. Ting, D. Hutchins, J.E. Baio, T.C. Lovejoy, A.H. Gage, D.G. Castner, H. Ma, A.K.Y. Jen, Simultaneous modification of bottom-contact electrode and dielectric surfaces for organic thin-film transistors through single-component spin-cast monolayers, Adv. Funct. Mater. 21 (2011) 1476–1488.
[23] S.Z. Weng, W.S. Hu, C.H. Kuo, Y.T. Tao, L.J. Fan, Y.W. Yang, Anisotropic field-effect mobility of pentacene thin-film transistor: effect of rubbed self-assembled monolayer, Appl. Phys. Lett. 89 (2006) 172103.
[24] W.H. Lee, J.H. Cho, K. Cho, Control of mesoscale and nanoscale ordering of organic semiconductors at the gate dielectric/semiconductor interface for organic transistors, J. Mater. Chem. 20 (2010) 2549–2561.
[25] O. Acton, G.G. Ting II, H. Ma, D. Hutchins, Y. Wang, B. Purushothaman, J.E. Anthony, A.K.Y. Jen, Π-σ-Phosphonic acid organic monolayer–amorphous sol–gel hafnium oxide hybrid dielectric for low-voltage organic transistors on plastic, J. Mater. Chem. 19 (2009) 7929–7936.
[26] W.Y. Chou, C.W. Kuo, H.L. Cheng, Y.R. Chen, F.C. Tang, F.Y. Yang, D.Y. Shu, C.C. Liao, Effect of surface free energy in gate dielectric in pentacene thin-film transistors, Appl. Phys. Lett. 89 (2006) 112126.
[27] S.K. Kim, S.Y. Yang, K. Shin, H. Jeon, J.W. Lee, K.P. Hong, C.E. Park, Low-operating-voltage pentacene field-effect transistor with a high-dielectric-constant polymeric gate dielectric, Appl. Phys. Lett. 89 (2006) 183516.
[28] S. Lee, B. Koo, J. Shin, E. Lee, H. Park, Effects of hydroxyl groups in polymeric dielectrics on organic transistor performance, Appl. Phys. Lett. 88 (2006) 162109.
[29] J. Gao, K. Asadi, J.B. Xu, J. An, Controlling of the surface energy of the gate dielectric in organic field-effect transistors by polymer blend, Appl. Phys. Lett. 94 (2009) 093302.
[30] J.X. Tang, C.S. Lee, M.Y. Chan, S.T. Lee, Enhanced electrical properties of pentacene-based organic thin-film transistors by modifying the gate insulator surface, Appl. Surf. Sci. 254 (2008) 7688–7692.
[31] H.S. Lee, K. Park, J.D. Kim, T. Han, K.H. Ryu, H.S. Lim, D.R. Lee, Y.J. Kwark, J.H. Cho, Interpenetrating polymer network dielectrics for high-performance organic field-effect transistors, J. Mater. Chem. 21 (2011) 6968–6974.
[32] J.W. Park, K.J. Baeg, J. Ghim, S.J. Kang, J.H. Park, D.Y. Kim, Effects of copper oxide/gold electrode as the source-drain electrodes in organic thin-film transistors, Electrochem. Solid-State Lett. 10 (2007) H340–H343.
[33] J. Veres, S. Ogier, G. Lloyd, Gate insulators in organic field-effect transistors, Chem. Mater. 16 (2004) 4543–4555.
[34] M.E. Roberts, N. Queraltó, S.C.B. Mannsfeld, B.N. Reinecke, W. Knoll, Z. Bao, Cross-linked polymer gate dielectric films for low-voltage organic transistors, Chem. Mater. 21 (2009) 2292–2299.
[35] C. Kim, Z. Wang, H.J. Choi, Y.G. Ha, A. Facchetti, T.J. Marks, Printable cross-linked polymer blend dielectrics. Design strategies, synthesis, microstructures, and electrical properties, with organic field-effect transistors as testbeds, J. Am. Chem. Soc. 130 (2008) 6867–6878.
[36] M.H. Yoon, H. Yan, A. Facchetti, T.J. Marks, Low-voltage organic field-effect transistors and inverters enabled by ultrathin cross-linked polymers as gate dielectrics, J. Am. Chem. Soc. 127 (2005) 10388–10395.
[37] S.Y. Yang, K. Shin, C.E. Park, The effect of gate-dielectric surface energy on pentacene morphology and organic field-effect transistor characteristics, Adv. Funct. Mater 15 (2005) 1806–1814.
[38] X. Sun, L. Zhang, C.A. Di, Y. Wen, Y. Guo, Y. Zhao, G. Yu, Y. Liu, Morphology optimization for the fabrication of high mobility thin-film transistors, Adv. Mater. 23 (2011) 3128–3133.
[39] T.B. Singh, F. Meghdadi, S. Günes, N. Marjanovic, G. Horowitz, P. Lang, S. Bauer, N.S. Sariciftci, High-performance ambipolar pentacene organic field-effect transistors on poly(vinyl alcohol) organic gate dielectric, Adv. Mater. 17 (2005) 2315–2320.
[40] Y. Wang, O. Acton, G. Ting, T. Weidner, H. Ma, D.G. Castner, A.K.Y. Jen, Low-voltage high-performance organic thin film transistors with a thermally annealed polystyrene/hafnium oxide dielectric, Appl. Phys. Lett. 95 (2009) 243302.
[41] H. Ma, O. Acton, G. Ting, J.W. Ka, H.L. Yip, N. Tucker, R. Schofield, A.K.Y. Jen, Low-voltage organic thin-film transistors with π-σ-phosphonic acid molecular dielectric monolayers, Appl. Phys. Lett. 92 (2008) 113303.
[42] Y. Wu, T. Toccoli, N. Koch, E. Iacob, A. Pallaoro, P. Rudolf, S. Iannotta, Elementary events of electron transfer in a voltage-driven quantum point contact, Phys. Rev. Lett. 98 (2007) 076601.
[43] S.E. Fritz, S.M. Martin, C.D. Frisbie, M.D. Ward, M.F. Toney, Structural characterization of a pentacene monolayer on an amorphous SiO_2 substrate with grazing incidence X-ray diffraction, J. Am. Chem. Soc. 126 (2004) 4084–4085.
[44] O.D. Jurchescu, M. Popinciuc, B.J. van Wees, T.T.M. Palstra, Interface-controlled, high-mobility organic transistors, Adv. Mater. 19 (2007) 688–692.
[45] H.L. Cheng, Y.S. Mai, W.Y. Chou, L.R. Chang, X.W. Liang, Thickness-dependent structural evolutions and growth models in relation to carrier transport properties in polycrystalline pentacene thin films, Adv. Funct. Mater. 17 (2007) 3639–3649.
[46] J.B. Brzoska, I.B. Azouz, F. Rondelez, Silanization of solid substrates: a step toward reproducibility, Langmuir 10 (1994) 4367–4373.
[47] A.N. Parikh, D.L. Allara, I.B. Azouz, F. Rondelez, An intrinsic relationship between molecular structure in self-assembled n-alkylsiloxane monolayers and deposition temperature, J. Phys. Chem. B 98 (1994) 7577–7590.
[48] R.R. Rye, Transition temperatures for n-alkyltrichlorosilane monolayers, Langmuir 13 (1997) 2588–2590.
[49] T. Suni, K. Henttinen, I. Suni, J. Mäkinen, Effects of plasma activation on hydrophilic bonding of Si and SiO_2, Electrochem. Soc. 149 (2002) G348.
[50] J.M. Ball, P.H. Wöbkenberg, F. Colléaux, M. Heeney, J.E. Anthony, I. McCulloch, D.D.C. Bradley, T.D. Anthopoulos, Solution processed low-voltage organic transistors and complementary inverters, Appl. Phys. Lett. 95 (2009) 103310.
[51] Y.A. Cheng, B. Zheng, P.H. Chuang, S. Hsieh, Solvent effects on molecular packing and tribological properties of octadecyltrichlo rosilane films on silicon, Langmuir 26 (2010) 8256–8261.